Materials Horizons

Accepted Manuscript

This article can be cited before page numbers have been issued, to do this please use: P. Han, C. Lin, K. Wang, Y. Qiu, H. Wu, A. Qin, D. Ma and B. Z. Tang, *Mater. Horiz.*, 2021, DOI: 10.1039/D1MH01129D.




ROYAL SOCIETY OF CHEMISTRY

rsc.li/materials-horizons

View Article Online
DOI: 10.1039/D1MH01129D

Triplet-triplet upconversion (TTU), where two low-energy triplet excitons are converted to one higher energy singlet exciton, is an excellent approach to break through the theoretical limit of the pure fluorescent organic light-emitting diodes (OLEDs) by 5%. To date, however, the reported emitters with high emission efficiency and excellent TTU efficiency in film state are rare. Herein, for the first time, we report an efficient non-doped blue OLED using the anthracene-based AIEgens with TTU process through spin-orbit coupling. The as-developed AIEgens exhibit high emission efficiency and excellent triplet upconversion efficiency close to 50% in film states, ultimately leading to the efficient blue TTU-OLED with external quantum efficiency of 8.1%. The excellent device performances suggest that the molecular design principle proposed herein is powerful for the development of TTU-OLEDs with high performance and low roll-off efficiency.

View Article Online
DOI: 10.1039/D1MH01129D

COMMUNICATION

# Aggregation-Induced Emission Luminogen with Excellent Triplet-Triplet Upconversion Efficiency for Highly Efficient Non-Doped Blue Organic Light-Emitting Diode

Received 00th January 20xx,
Accepted 00th January 20xx

DOI: 10.1039/x0xx00000x

Pengbo Han,[a] Chengwei Lin,[a] Kaojin Wang,[a] Yanping Qiu,[a] Haozhong Wu,[a] Anjun Qin*[a] Dongge Ma,*[a] and Ben Zhong Tang,*[ab]



**By combining aggregation-induced emission (AIE) effect and triplet-triplet upconversion (TTU) process, a blue emitter with excellent photoluminescence quantum efficiency and high upconversion efficiency in the film state is developed, from which a highly efficient non-doped blue TTU organic light-emitting diode (TTU-OLED) was realized.**

Organic light-emitting diodes (OLEDs) have been widely used in the field of full-color flat-panel displays and white lighting.[1] In OLEDs, injected electrons and holes recombine to form 25% singlet excitons and 75% triplet excitons.[2] Therefore, one of the most effective methods to enhance the efficiency of OLEDs requires the contribution from triplet excitons. Phosphorescent OLEDs (Ph-OLEDs) containing transition metal complexes can achieve 100% internal quantum efficiency (IQE) through strong spin-orbit coupling effect of heavy atoms.[3] Alternatively, the lowest triplet ($T_1$) excitons can be up-converted to singlet ($S_1$) ones through reverse intersystem crossing (RISC) process to realize thermally activated delayed fluorescence (TADF)[4], leading to a nearly 100% IQE.[5] Although blue Ph- and TADF-OLEDs can harvest triplet excitons efficiently, their operation lifetime and efficiency roll-off in high voltage are still a hindrance due to their long exciton lifetime and high triplet energy levels.[6] Meanwhile, low $T_1$ excitons can be theoretically converted into high $S_1$ state through triplet fusion (TF) process to make use of triplet excitons.[7] Triplet-triplet upconversion (TTU) OLEDs can not only achieve a high IQE, but also possess long operation lifetime compared with blue TADF and Ph-OLEDs.[8] Therefore, it is highly desirable to develop efficient blue TTU-OLEDs.

As shown in Fig. 1A, two triplet fusion generates an intermediate state ($T_1$+$T_1$), whose spin-spin coupling leads to the formation of 1/9 singlet $^1(TT)$, 1/3 triplet $^3(TT)$, and 5/9 quintet $^5(TT)$.[9] The $^1(TT)$ and $^3(TT)$ can form $S_1$ and $T_1$ with a molecular ground state ($S_0$), respectively. Conversely, $^5(TT)$ could be up-converted to $T_1$+$T_1$ intermediate state, because its energy is lower than that of quintet (intramolecular) excited state ($Q_1$).[8c] Therefore, $T_1$ can form $S_0$ by the repeated TF process with a upconversion efficiency ($\eta_{TTU}$) of close to 20%.[9a] When the energy level of $T_2$ is higher than that of $2T_1$, $^3(TT)$ can be expected to return directly to $2T_1$, and the $\eta_{TTU}$ can be also raised to 50%.[10] However, the high TF efficiency is only limited to some special materials, such as anthracene derivatives and rubrene, because of the strict energetic requirements.[8a,11] Alternatively, the transition from $^3(TT)$ to $S_1$ has been suggested to break through the limit of $\eta_{TTU}$.[12] Although it is a promising pathway to improve $\eta_{TTU}$, blue OLED with high-performance based on the transitions is rare because of the absence of effective molecular design strategy.

9,10-diphenylanthracene (DPA), a polycyclic aromatic hydrocarbon (PAH) compound with low triplet energy level and good stability, is typically used as an emitter for the construction of blue TTU OLEDs.[13] In principle, TTU is a bimolecular process and needs high enough triplet exciton concentration to improve TF efficiency. However, DPA is usually doped into appropriate host materials due to its aggregation-caused quenching (ACQ) effect.[14] As a result, it is difficult for the doped devices to achieve high-performance blue OLEDs by controlling TF process. More importantly, it is complicated to prepare the doped devices. Therefore, developing PAH compounds with intense film state emission is beneficial for the construction of high-performance non-doped blue TTU-OLEDs.

Exactly opposite to the ACQ effect, the luminogens with aggregation-induced emission characteristics (AIEgens) can exhibit intense emission in their film states.[15] Thus, they are ideal candidates to combine PAH compounds with TTU feature

[a] State Key Laboratory of Luminescent Materials and Devices, Guangdong Provincial Key Laboratory of Luminescence from Molecular Aggregates, Center for Aggregation-Induced Emission, South China University of Technology, Guangzhou, Guangdong 510640, China. E-mail: msdgma@scut.edu.cn; msqinaj@scut.edu.cn
[b] Shenzhen Institute of Molecular Aggregate Science and Engineering, School of Science and Engineering, The Chinese University of Hong Kong, Shenzhen, 2001 Longxiang Boulevard, Longgang District, Shenzhen City, Guangdong 518172, China. E-mail: tangbenz@cuhk.edu.cn

†Electronic Supplementary Information (ESI) available. CCDC 2042010. For ESI and crystallographic data in CIF or electronic format See DOI: 10.1039/x0xx00000x

View Article Online
DOI: 10.1039/D1MH01139D

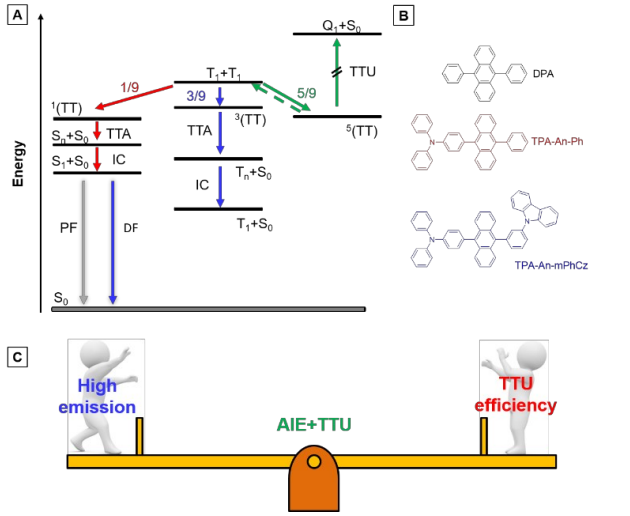


**Fig. 1** (A) Energy-level diagram illustrating the mechanisms of triplet-triplet upconversion (TTU) and triplet-triplet annihilation (TTA). $^1(TT)$, $^3(TT)$, and $^5(TT)$ are singlet, triplet, and quintet intermediate states. $S_1$, $T_1$, and $S_0$ are singlet excitons, triplet excitons, and ground states. $S_n$ and $T_n$ are higher singlet and triplet states. (B) Chemical structures of the anthracene derivatives. (C) Design principle of blue emitters.

to solve above problems. According to our reported design strategy, new AIEgens, decorating ACQ molecules with triphenylamine (TPA) moiety, have also been achieved.[16] In addition, Konishi *et al.* illustrated that the frontier orbitals of diarylamine and anthracene interpenetrated when the planar donor was distorted,[17] meanwhile, a transition between molecular orbitals with relative orthogonal directions might also promote the conversion process from $^3(TT)$ to $S_1$.[12]

Herein, the compounds TPA-An-Ph and TPA-An-mPhCz, in which the twisted donating groups of triphenylamine (TPA) was attached on anthracene (An) cores together with the meta-positions substituted planar group of carbazole (Cz) group in the latter, were designed and synthesized (Fig. 1B). The carbazole group can facilitate the hole transport of devices, which in turn improve the device performance.[18] In addition, it was demonstrated that high-efficiency solid-state emission can be achieved by the meta-substituted strategy.[19] Thanks to their AIE feature, TPA-An-Ph and TPA-Ph-mPhCz show high photoluminescence quantum efficiency yields (PLQYs, $\Phi_F$) in their film states. The non-doped OLEDs using these AIEgens as emitting layers (EMLs) show blue emission and exhibit low efficiency roll off. The TPA-An-Ph-based OLED gives a maximum forward-viewing external quantum efficiency (EQE) of 4.51%. Notably, the TPA-An-mPhCz-based OLED achieves a maximum EQE of 8.1%. The transient electroluminescence (EL) spectra and theoretical calculation suggest that this could be ascribed to the effective TTU conversion process from $^3(TT)$ to $S_n$ of TPA-An-mPhCz. This strategy might provide an instructive way to achieve highly efficient commercialized blue OLEDs by the construction of AIEgens with effective TTU process (Fig. 1C).

The synthetic routes to TPA-An-Ph and TPA-An-mPhCz are shown in Scheme S1. They could be facilely synthesized in 80% yields by the Suzuki coupling reaction. The structures of TPA-An-Ph and TPA-An-mPhCz were fully characterized by $^1$H and $^{13}$C NMR and high resolution mass (HRMS) spectroscopies. For comparison, the commercialized DPA was used to explore the rationality of the design. DPA, TPA-An-Ph and TPA-An-mPhCz are soluble in commonly used organic solvents, such as dichloromethane (DCM) and tetrahydrofuran (THF), but insoluble in water.

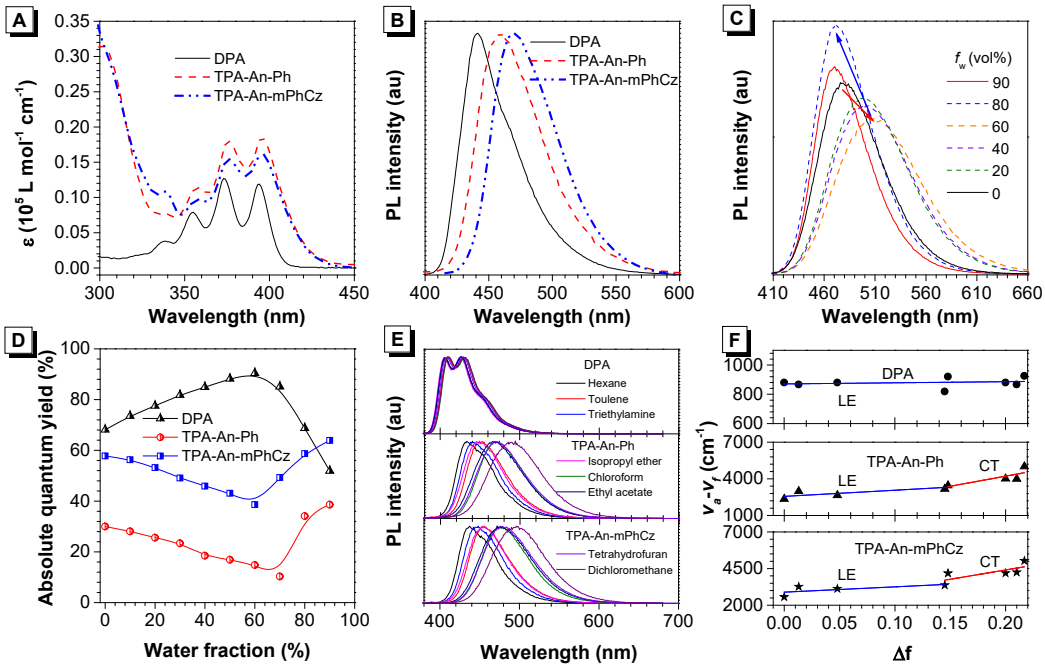


**Fig. 2** (A) UV-vis (THF solution) and (B) photoluminescence (PL, film state) spectra of DPA, TPA-An-Ph, and TPA-An-mPhCz. (C) PL spectra of TPA-An-mPhCz in THF/water mixtures with different water fractions ($f_w$); $\lambda_{ex}$: 360 nm; concentration: 10 μM. (D) Absolute photoluminescence quantum yield of DPA, TPA-An-Ph, and TPA-An-mPhCz versus water fractions in THF/water mixtures. (E) Effects of solvent on fluorescence spectra of the anthracene derivatives. (F) Stokes shifts of the anthracene derivatives as a function of the orientation polarizability. The solid lines are the fitting results by the Lippert-Mataga equation.

After confirming their structures, the photophysical properties of DPA, TPA-An-Ph and TPA-An-mPhCz were studied. Fig. 2A shows their ultraviolet-visible (UV-Vis) absorption spectra in THF solutions. The absorption band at 360-400 nm could readily be assigned to the π-π* transition of the anthracene core.[20] The PL spectra of DPA, TPA-An-Ph and TPA-An-mPhCz in THF solutions exhibit deep blue and blue emissions with peaks ranging from 409 to 476 nm upon photoexcitation (Fig. S1, ESI†). In comparison with DPA in THF solution, the emission peaks of TPA-An-Ph and TPA-An-mPhCz were considerably red-shifted because of the enlongation of the conjugation. Meanwhile, featureless PL spectra were obtained for TPA-An-Ph and TPA-An-mPhCz in THF solutions, implying that each emission originates from charge transfer (CT) state. The PL spectra of the vacuum-deposited neat films of DPA, TPA-An-Ph, and TPA-An-mPhCz show deep blue and blue emission with peaks at 442, 460 and 470 nm, respectively (Fig. 2B). The $\Phi_F$ value of DPA in THF solution was 68.1%, but reduced to 59.3% in vacuum-deposited neat film. Notably, $\Phi_F$ values of TPA-An-Ph and TPA-An-mPhCz in THF solutions were measured to be 30.0 and 57.8%, and further enhanced to 40.1% and 65.1% in their vacuum-deposited neat films, respectively. These results suggest that TPA-An-Ph and TPA-An-mPhCz exhibit the aggregation-enhanced emission (AEE) feature.

To further explore the AEE feature of TPA-An-Ph and TPA-An-mPhCz, their PL behaviors was explored in THF/water mixtures with different water fractions ($f_w$). As shown in Fig. 2C and S2, the emission peaks slowly red-shifted along with the decrease in PL intensity when $f_w$ was gradually increased, which is attributed to the process of twisted intramolecular charge transfer (TICT).[21] However, when the $f_w$ was further increased, their PL gradually intensified along with blue-shifted emission peak owing to the formation of aggregates and activation of restriction of intramolecular motion (RIM).[22] In contrast with TPA-An-Ph and TPA-An-mPhCz, the $\Phi_F$ values of DPA in THF/water mixtures with different $f_w$ shows completely opposite trend (Fig. 2D), further demonstrated the effectiveness of our design strategy.

To concretely analyze excited states of DPA, TPA-An-Ph and TPA-An-mPhCz, their PL spectra were investigated in different solvents (Fig. 2E). According to the Lippert-Mataga model,[23] the dipole moments of their excited state can be acquired by a slope of the Stokes shift ($\nu_a$-$\nu_f$) as a function of the orientation polarizability ($f$) as shown in Tables S1-S3 (ESI†). The fitting results are shown in Fig. 2F. The derived dipole moment ($\mu_e$) of the excited state of DPA is 0.69 D, indicating that its excited state could be assigned to localized excited (LE) states. While, TPA-An-Ph and TPA-An-mPhCz exhibit the two independent slops: smaller $\mu_e$ values of 7.27 and 9.02 D in low polar solvents and larger $\mu_e$ values of 12.93 and 14.95 D in highly polar solvents, respectively. These results suggest that their excited states are assigned to LE and CT states, respectively. Furthermore, their PL spectra in film state were measured at 77 K (Fig. S3, ESI†), and the peaks of DPA, TPA-An-Ph and TPA-An-mPhCz were recorded to be 424 nm (2.92 eV), 454 nm (2.73 eV), and 467 nm (2.66 eV), respectively. The PL spectra of TPA-An-Ph and TPA-An-mPhCz in film state are close to those in polar solvents rather than those in nonpolar solvents. Therefore, the $S_1$ states of TPA-An-Ph and TPA-An-mPhCz films would be assigned to a $^1$CT mixing weak $^1$LE state. Moreover, the PL decay curves of DPA, TPA-An-Ph and TPA-An-mPhCz were plotted in Fig. S4 (ESI†). Their lifetime shows a single-exponential decay process in THF solutions and solid films, suggesting that they emit fluorescence.

To have a deeper understanding of the structure-property relationships, the single crystal of TPA-An-mPhCz (CCDC 2042010) was obtained by solvent evaporation method and analyzed by X-ray diffraction crystallography. As shown in Fig. 3A, TPA-An-mPhCz possesses a highly twisted L-shape molecular configuration with large dihedral angles distributing between 61° and 81°. Moreover, strong multiple intermolecular C-H···π hydrogen bonds with a short distances of 2.702-3.721 Å are found between the molecules (Fig. 3B). Notably, no close π-π stacking interaction was found in Fig. 3C and 3D. These factors can effectively rigidify molecular conformation and reduce non-radiative energy dissipation in the aggregate state, resulting in an AEE effect.[24]

Besides their high $\Phi_F$ values in the film states, TPA-An-Ph and TPA-An-mPhCz are thermally stable according to the differential scanning calorimetry (DSC) and thermogravimetric analysis (TGA) measurement. As depicted in Fig. S5 and Table S4 (ESI†), the decomposition temperatures ($T_d$, 5% weight loss) of TPA-An-Ph and TPA-An-mPhCz are 362 and 411 °C, respectively, and no glass transition temperatures ($T_g$) were found in the measurement region. These results suggest that they are suitable for the preparation of vapor deposition device. In addition, the electrochemical properties of TPA-An-Ph and TPA-An-mPhCz were measured by using cyclic voltammetry (CV). As shown in Fig. S6 (ESI†), the highest occupied molecular orbital (HOMO) energy levels of TPA-An-Ph and TPA-An-mPhCz

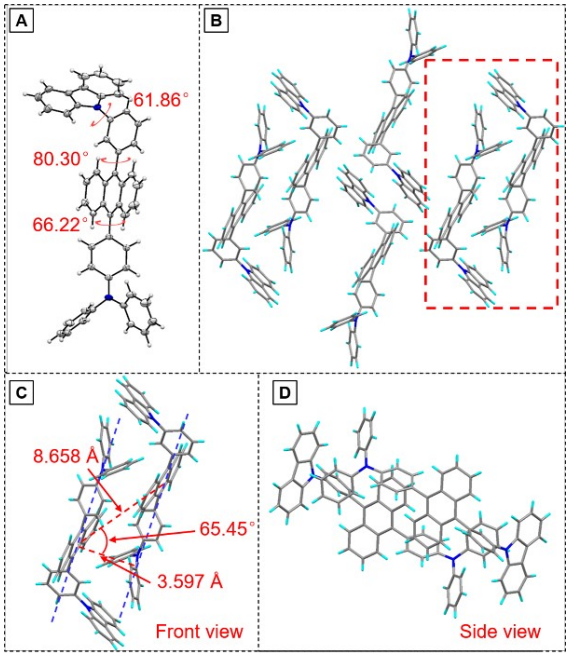


**Fig. 3** (A) Crystal structure and (B) packing pattern of **TPA-An-mPhCz** in single crystals; (C) front view and (D) side view of the detailed molecular stacking with red dotted line.

View Article Online
DOI: 10.1039/D1MH01129D

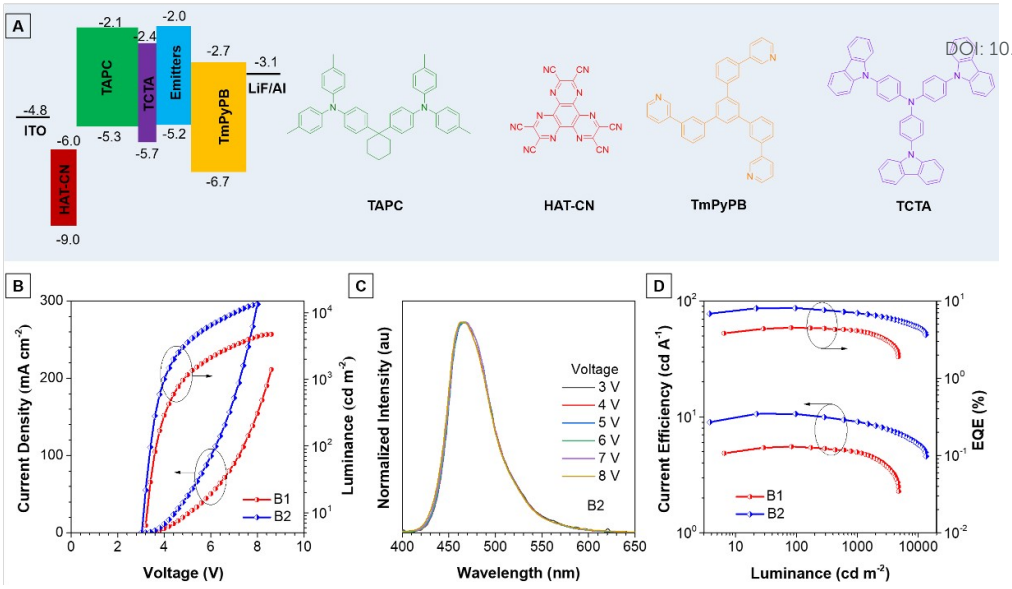


**Fig. 4** (A) Device structure and ionization potentials (IPCV) and electron affinities (EACV) for each material. (B) Current density-voltage-luminance (J-V-L) characteristics of devices B1 and B2. (C) Electroluminescence (EL) spectra of device B2 at various voltages. (D) CE and EQE versus luminance curves of the non-doped OLEDs based on AIEgens of TPA-An-P**h** and TPA-An-mPhCz.

are deduced to be -5.20 and -5.22 eV, and thier lowest unoccupied molecular orbital (LUMO) energy levels are -2.51 and -2.52 eV, respectively, which will facilitate the device configuration optimization.

Thanks to the excellent thermal stability and the high emission efficiency in aggregate/film states, the non-doped devices B1 and B2 were constructed by using TPA-An-Ph and TPA-An-mPhCz as EMLs, respectively, with a device configuration of ITO/HAT-CN (5 nm)/TAPC (60 nm)/TCTA (5 nm)/EMLs (20 nm)/TmPyPB (40 nm)/LiF (1 nm)/Al (Fig. 4A), where ITO, 1,4,5,8,9,11-hexaazatriphenylene-hexacarbonitrile (HAT-CN), 1-bis[4-[N,N-di(4-tolyl)amino]-phenyl]-cyclo-hexane (TAPC), 4,4',4''-tri(*N*-carbazolyl)-triphenylamine (TCTA), and 1,3,5-tri[(3-pyridyl)-phen-3-yl]benzene (TmPyPB) act as the anode, hole injection, hole-transporting, exciton-blocking layers, and electron-transporting layers, respectively. These non-doped OLEDs emit blue light and exhibit excellent device performance at low operation voltages (Fig. 4B). It is worth noting that the EL spectra keep stable when the voltage increased from 3 to 8 V, confirming their good color stability (Fig. 4C and S7, ESI†). Moreover, device B2 presents an emission peak at 470 nm with a narrow full width at half-maximum (FWHM) of 58 nm, which is useful for blue emission of OLEDs. As depicted in Fig. 4D, device B1 achieves a maximum forward-viewing EQE of 4.51% and CE of 5.54 cd/A. Whereas, B2 gives a maximum EQE of 8.10% and CE of 10.62 cd/A. More importantly, the EQE and CE of B2 also remain high values of 6.97% and 9.09 cd/A at a luminance of 1000 cd $m^{-2}$, demonstrating the low efficiency roll-off of the device. Meanwhile, the power efficiency of these devices shows identical result (Fig. S8 and Table S5, ESI†).

Meanwhile, the doped devices were also fabricated with a configuration of ITO/HAT-CN (5 nm)/TAPC (60 nm)/TCTA (5 nm)/EML (20 nm)/TmPyPB (40 nm)/LiF (1 nm)/Al using 2,6-bis(3-(9H-carbazol-9-yl)phenyl)pyridine (26DCZPPy) as host and TPA-An-mPhCz as guest with different doping concentrations (device 1: 10%, device 2: 20%, and device 3: 50%. As shown in Table S6 (ESI†), the TPA-An-mPhCz based doped devices show blue emission with EL peaks at 458, 462 and 474 nm at low operation voltages, respectively (Fig. S9A and S9B, ESI†). Among the fabricated doped OLEDs, device 3 achieves a maximum EQE of 5.60%, CE of 7.82% and PE of 5.85%. These EL spectra keep stable when the voltage increased from 4 to 7 V, confirming their good color stability (Fig. S10, ESI†). However, these values are far behind those of device B2 (Fig. S9C, S9D and S11, ESI†), suggesting the advantages of non-doped OLEDs using AIEgens as EMLs.

It is worth noting that the EQE of device B2 breaks through the theoretical limit (5%) of the pure fluorescent OLEDs. Theoretically, the EQE equals to $\eta_{eh} \times \eta_{PL} \times \eta_{exciton} \times \eta_{out}$, where $\eta_{eh}$ is the factor of the recombination efficiency of injected holes and electrons (ideally 100%), $\eta_{PL}$ is the absolute $\Phi_F$ of emitter (65.1% for the vacuum evaporated films of TPA-An-mPhCz), $\eta_{exciton}$ is the radiative exciton ratio, and $\eta_{out}$ is the light out-coupling efficiency. We measured angle-dependent PL of TPA-An-mPhCz, but no data were obtained. Therefore, $\eta_{out}$ is assumed to be 20%. According to the above equation, $\eta_{exciton}$ of the non-doped OLED is calculated to be 62.2% by using TPA-An-mPhCz as EML, suggestive of the involved triplet excitons in the radiative process.

To verify the improved mechanism in EL efficiency of TPB-An-mPhCz-based OLED, we first measured the fluorescence lifetime of TPA-An-mPhCz film, which shows a single-exponential decay process with the value of 3.58 ns. Then, we obtained its $T_1$ energy level by measuring its phosphorescent spectrum according the reported method,[20] which is deduced to be 1.76 eV (Fig. S12, ESI†). These results suggest that TPA-An-mPhCz possesses a large energy gap between $S_1$ and $T_1$. Therefore, TADF is excluded for the high performance OLED.

View Article Online DOI: 10.1039/D1MH01129D

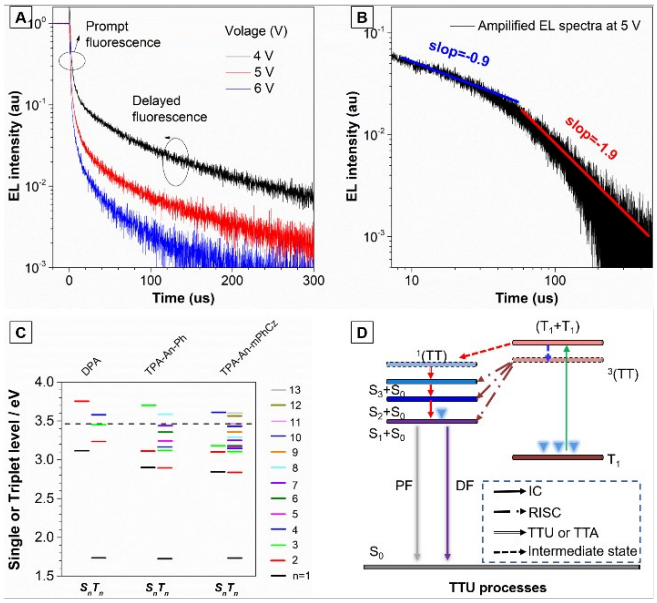


**Fig. 5** (A) Transient EL decay of the non-doped device B2 at different voltages. (B) Amplified EL spectra of the non-doped device B2 at 5 V. (C) Energy diagrams. Energy levels and twice the $T_1$ energies (dashed line) of the anthracene derivatives calculated using B3LYP/6-311G(d,p), where n is the quantum number used to indicate the excited state. (D) Proposed TTU mechanism based on the emitters.

Next, the transient EL decay of the non-doped device at different voltages were analyzed. As shown in Fig. 5A, the EL decay exhibits two parts, the prompt fluorescence and the delayed fluorescence. Triplet excitons return directly to higher excited singlet states, which results in no delayed component in transient EL spectra of hybridized local and charge transfer (HLCT)-OLEDs.[23] Thus, the emission mechanism should be TTU. The prompt part originates from singlet exciton emission under electrical pumping, and the following delayed component is attributed to triplet excitons via the TF process. Moreover, the ratio of delayed fluorescence slowly decreases with increasing voltage. It is hypothesized that the delayed portion is not simply from the recombination of the trapped charges.[11b] As reported by Kondakov et al., the delayed EL is proportional to $t^{-2}$ ($t$ is the time) when TTU is predominant in OLED.[25] The plot of Log(EL intensity) versus log($t$) for device B2 is shown in Fig. 5B. The slope of the obtained curve is nearly -2, which is consistent with TTU-related triplet exciton dynamics as described above, further confirming the existence of TTU process in TPA-An-mPhCz-based OLED.

To further confirm our assumption, the excited states of DPA, TPA-An-Ph, and TPA-An-mPhCz were calculated by TD-DFT calculations based on B3LYP/6-311(d,p) basis set. As shown in Fig. 5C, the $T_1$ energy levels of DPA, TPA-An-Ph and TPA-An-mPhCz are all close to 1.73 eV, which are consistent with the results reported in the literature and were derived from the $^3$LE state of the anthracene unit.[26] Thus, their $^3(TT)$ are almost identical. In addition, the energy of $2T_1$ is higher than $T_2$, indicating that $\eta_{TTU}$ is close to 20% and in turn leading to $\eta_{exciton}$ of 32.5%. However, the scenario cannot explain the maximum EQE of TPA-An-mPhCz based OLED. Therefore, the possibility of a conversion process from $^3(TT)$ to $S_n$ ($\leq 3$) should be considered. According to previous work[12], the spin-orbit interaction between $S_n$ and $T_m$ whose energy levels are close to that of $^3(TT)$ and in the range of 3.40-3.50 eV (Table S7, ESI†), should be taken into account. The TTU transition would form $S_n$ and then return to $S_1$ via internal conversion. The possible TTU transition from $^3(TT)$ to $S_n$ are given in Table S8 (ESI†). For TPA-An-Ph (Fig. S13, ESI†) and TPA-An-mPhCz (Fig. S14, ESI†), the TTU transition involves different vectors of the magnetic moments. For example, as depicted in Fig. S14 (ESI†) and Table S8 (ESI†), the spin-orbit matrix of $\langle S_3 | H_{so} | T_{10} \rangle$ consisting of HOMO-2 and HOMO-4 are involved in the TTU transition from $^3(TT)$ to $S_n$ for TPA-An-mPhCz. The HOMO-4 is localized on the anthracene unit, whereas HOMO-2 is mainly localized on the carbazole unit, which is oriented perpendicularly to the anthracene unit. As a result, the rotation of the molecular orbitals from the carbazole unit to the anthracene unit is involved in the spin-orbit matrices, leading to TTU process according to spin conversion, as illustrated in Fig. 4D. This process is different from HLCT and "Hot" exciton process because the observed delayed fluorescence in OLEDs is derived from the TTU process.

## Conclusions

Novel blue AIEgens of TPA-An-Ph and TPA-An-mPhCZ were designed and synthesized. They show excellent thermal stability and high $\Phi_F$ in their film states. The non-doped OLEDs exhibit excellent device performance. The maximum CE and EQE of TPA-An-mPhCz-based OLED can reach up to 10.62 cd/A and 8.10%, respectively, with an operation voltage as low as 3.0 V. More importantly, the CE and EQE still remain high values of 9.09 cd/A and 6.97%, respectively, at a luminance of 1000 cd m$^{-2}$, suggestive of low efficiency roll-off of the device. The transient EL spectrum and theoretical calculation confirm that the unique TTU process of the emitter plays a crucial role in achieving high EQE. The design strategy of combination of TTU process and AIE effect is valuable for the construction of high-performance OLEDs, which might be beneficial for practical applications, such as white lighting and full color flat-panel displays.

## Author Contributions

P. Han, A. Qin and B. Z. Tang conceived the original idea for investigation. P. Han, K. Wang, A. Qin and B. Z. Tang wrote the manuscript. P. Han synthesized the compounds. P. Han, and Y. Qiu measured the photophysical, thermal and electrochemical properties of the compounds. C. Lin and D. Ma fabricated characterized the devices. P. Han performed the X-ray single crystal diffraction analysis. P. Han and H. Wu performed the quantum chemical calculations. All authors discussed the progress of research and reviewed the manuscript.

## Conflicts of interest

There are no conflicts to declare.

View Article Online
DOI: 10.1039/D1MH01250D

## Acknowledgements

This work was financially supported by the National Natural Science Foundation of China (21788102), the Natural Science Foundation of Guangdong Province (2019B030301003 and 2016A030312002), and the Innovation and Technology Commission of Hong Kong (ITC-CNERC14S01).

## References

1 (a) C. W. Tang and S. A. VanSlyke, *Appl. Phys. Lett.,* 1987, **51**, 913-915; (b) J. Kido, M. Kimura, K. Nagai, *Science,* 1995, **267**, 1332-1334; (c) Y. Sun, N. C. Giebink, H. Kanno, B. Ma, M. E. Thompson and S. R. Forrest, *Nature,* 2006, **440**, 908-912.
2 W. Helfrich and W. G. Schneider, *J. Chem. Phys.,* 1966, **44**, 2902-2909.
3 (a) H. Kuo, Y. Chen, L. R. Devereux, C. Wu, M. A. Fox, C. Kuei, Y. Chi and G. Lee, *Adv. Mater.,* 2017, **29**, 1702464; (b) C. Adachi, M. A. Baldo, M. E. Thompson and S. R. Forrest, *J Appl. Phys.,* 2001, **90**, 5048-5051.
4 A. Endo, M. Ogasawara, A. Takahashi, D. Yokoyama, Y. Kato and C. Adachi, *Adv. Mater.,* 2009, **21**, 4802-4806.
5 H. Uoyama, K. Goushi, K. Shizu, H. Nomura and C. Adachi, *Nature,* 2012, **492**, 234-238.
6 (a) J. U. Kim, I. S. Park, C. Chan, M. Tanaka, Y. Tsuchiya, H. Nakanotani and C. Adachi, *Nat. Commun.,* 2020, **11**, 1-8; (b) K. Tuong Ly, R. Chen-Cheng, H. Lin, Y. Shiau, S. Liu, P. Chou, C. Tsao, Y. Huang and Y. Chi, *Nat. Photonics,* 2017, **11**, 63-68; (c) J. Lee, C. Chen, P. Lee, H. Lin, M. Leung, T. Chiu and C. Lin, *J. Mater. Chem. C,* 2019, **7**, 5874-5888.
7 (a) C. Ganzorig and M. Fujihira, *Appl. Phys. Lett.,* 2002, **81**, 3137-3139; (b) D. Y. Kondakov, T. D. Pawlik, T. K. Hatwar and J. P. Spindler, *J. Appl. Phys.,* 2009, **106**, 124510.
8 (a) A. Salehi, C. Dong, D. Shin, L. Zhu, C. Papa, A. Thy Bui, F. N. Castellano and F. So, *Nat. Commun.,* 2019, **10**, 1-9; (b) J. Huh, Y. H. Ha, S. Kwon, Y. Kim and J. Kim, *ACS Appl. Mater. Interfaces,* 2020, **12**, 15422-15429; (c) X. Qiao and D. Ma, *Mater. Sci. Eng. R,* 2020, **139**, 100519.
9 (a) C. Chiang, A. Kimyonok, M. K. Etherington, G. C. Griffiths, V. Jankus, F. Turksoy and A. P. Monkman, *Adv. Funct. Mater.,* 2013, **23**, 739-746; (b) T. L. Keevers and D. R. McCamey, *Phys. Rev. B,* 2016, **93**, 045210; (c) B. H. Wallikewitz, D. Kabra, S. Gélinas and R. H. Friend, *Phys. Rev. B,* 2012, **85**, 045209.
10 Y. Y. Cheng, T. Khoury, R. G. C. R. Clady, M. J. Y. Tayebjee, N. J. Ekins-Daukes, M. J. Crossley and T. W. Schmidt, *Phys. Chem. Chem. Phys.,* 2010, **12**, 66-71.
11 (a) D. Di, L. Yang, J. M. Richter, L. Meraldi, R. M. Altamimi, A. Y. Alyamani, D. Credgington, K. P. Musselman, J. L. MacManus-Driscoll and R. H. Friend, *Adv. Mater.* 2017, **29**, 1605987; (b) W. Liu, S. Ying, R. Guo, X. Qiao, P. Leng, Q. Zhang, Y. Wang, D. Ma and L. Wang, *J. Mater. Chem. C* 2019, **7**, 1014-1021.
12 R. Ieuji, K. Goushi, C. Adachi, *Nat. Commun.,* 2019, **10**, 5283.
13 R. Sato, H. Kitoh-Nishioka, K. Kamada, T. Mizokuro, K. Kobayashi and Y. Shigeta, *J. Phys. Chem. C,* 2018, **122**, 5334-5340.
14 J. Yang, Z. Chi, W. Zhu, B. Z. Tang and Z. Li, *Sci. China Chem.,* 2019, **62**, 1090-1098.
15 (a) Z. Zhao, H. Zhang, J. W. Y. Lam and B. Z. Tang, *Angew. Chem., Int. Ed.,* 2020, **59**, 2-22; (b) J. Yang, M. Fang and Z. Li, *Aggregate*, 2020, **1**, 6-18.
16 J. Mei, N. L. C. Leung, R. T. K. Kwok, J. W. Y. Lam and B. Z. Tang, *Chem. Rev.,* 2015, **115**, 11718-11940.
17 S. Sasaki, S. Suzuki, W. M. C. Sameera, K. Igawa, K. Morokuma and G. Konishi, *J. Am. Chem. Soc.* 2016, **138**, 8194-8206.
18 P. Han, C. Lin, D. Ma, A. Qin, B. Z. Tang, *ACS Appl. Mater. Inter.,* 2020, **12**, 46366-46372.
19 H. Liu, D. Cong, B. Li, L. Ye, Y. Ge, X. Tang, Y. Shen, Y. Wen, J. Wang, C. Zhou and B. Yang, *Cryst. Growth Des.*, 2017, **17**, 2945-2949.
20 X. Tang, Q. Bai, T. Shan, J. Li, Y. Gao, F. Liu, H. Liu, Q. Peng, B. Yang, F. Li and P. Lu, *Adv. Funct. Mater.,* 2018, **28**, 1705813.
21 R. Hu, E. Lager, A. Aguilar-Aguilar, J. Liu, J. W. Y. Lam, H. H. Y. Sung, I. D. Williams, Y. Zhong, K. S. Wong, E. Peña-Cabrera and B. Z. Tang, *J. Phys. Chem. C,* 2009, **113**, 15845-15853.
22 H. Nie, K. Hu, Y. Cai, Q. Peng, Z. Zhao, R. Hu, J. Chen, S. Su, A. Qin and B. Z. Tang, *Mater. Chem. Front.,* 2017, **1**, 1125-1129.
23 W. Li, Y. Pan, L. Yao, H. Liu, S. Zhang, C. Wang, F. Shen, P. Lu, B. Yang and Y. Ma, *Adv. Opt. Mater.,* 2014, **2**, 892-901.
24 J. Guo, X. Li, H. Nie, W. Luo, S. Gan, S. Hu, R. Hu, A. Qin, Z. Zhao, S. Su and B. Z. Tang, *Adv. Funct. Mater.,* 2017, **27**, 1606458.
25 D. Y. Kondakov, J. Appl. Phys., 2007, **102**, 114504.
26 S. Reineke and M. A. Baldo, *Sci. Rep.,* 2014, **4**, 3797.





 